

Efficient estimation of the ANOVA mean dimension, with an application to neural net classification

Christopher Hoyt Art B. Owen
Stanford University Stanford University

July 2020

Abstract

The mean dimension of a black box function of d variables is a convenient way to summarize the extent to which it is dominated by high or low order interactions. It is expressed in terms of $2^d - 1$ variance components but it can be written as the sum of d Sobol' indices that can be estimated by leave one out methods. We compare the variance of these leave one out methods: a Gibbs sampler called winding stairs, a radial sampler that changes each variable one at a time from a baseline, and a naive sampler that never reuses function evaluations and so costs about double the other methods. For an additive function the radial and winding stairs are most efficient. For a multiplicative function the naive method can easily be most efficient if the factors have high kurtosis. As an illustration we consider the mean dimension of a neural network classifier of digits from the MNIST data set. The classifier is a function of 784 pixels. For that problem, winding stairs is the best algorithm. We find that inputs to the final softmax layer have mean dimensions ranging from 1.35 to 2.0.

Keywords: chaining, explainable AI, global sensitivity analysis, pick-freeze, Sobol' indices, winding stairs

1 Introduction

The mean dimension of a square integrable function quantifies the extent to which higher order interactions among its d input variables are important. At one extreme, an additive function has mean dimension one and this makes numerical tasks such as optimization and integration much simpler. It can also make it easier to compare the importance of the inputs to a function and it simplifies some visualizations. At the other extreme, a function that equals a d -fold interaction has mean dimension d and can be much more difficult to study.

The mean dimension of a function can be estimated numerically by algorithms that change just one input variable at a time. A prominent example is the winding stairs estimator of Jansen et al. (1994) which runs a Gibbs sampler over the input space. The squared differences in a function’s value arising from changing one input at a time can be used to estimate a certain Sobol’ index described below. The mean dimension is defined in terms of a sum of such Sobol’ indices. When estimating the mean dimension, covariances among the corresponding Sobol’ estimates can greatly affect the efficiency of the estimation strategy. Sometimes a naive approach that uses roughly twice as many function evaluations can be more efficient than winding stairs because it eliminates $O(d^2)$ covariances.

The outline of this paper is as follows. Section 2 introduces some notation, and defines the ANOVA decomposition, Sobol’ indices and the mean dimension. Section 3 presents three strategies for sampling pairs of input points that differ in just one component. A naive method takes $2Nd$ function evaluations to get N such pairs of points for each of d input variables. It never reuses any function values. A radial strategy (Campolongo et al., 2011) uses $N(d + 1)$ function evaluations in which N baseline points each get paired with d other points that change one of the inputs. The third strategy is winding stairs mentioned above which uses $Nd + 1$ function evaluations. Section 4 compares the variances of mean dimension estimates based on these strategies. Those variances involve fourth moments of the original function. We consider additive and multiplicative functions. For additive functions all three methods have the same variance making the naive method inefficient by a factor of about 2 for large d . For more complicated functions, methods that save function evaluations by reusing some of them can introduce positive correlations yielding a less efficient estimate. The presence of high kurtoses can decrease the value of reusing evaluations. Section 5 presents an example where we measure the mean dimension of a neural network classifier designed to predict a digit 0 through 9 based on 784 pixels. We find some mean dimensions in the range 1.35 to 2.0 for the penultimate layer of the network, suggesting that the information from those pixels is being used mostly one or two or three at a time. For instance, there cannot be any meaningfully large interactions of 100 or more inputs. Section 6 makes some concluding remarks. Notably, the circumstances that make the radial method inferior to the naive method or winding stairs for computing mean dimension serve to make it superior to them for some other uncertainty quantification tasks. We also discuss randomized quasi-Monte Carlo sampling alternatives. Finally, there is an Appendix in which we make a more detailed analysis of winding stairs.

2 Notation

We begin with the analysis of variance (ANOVA) decomposition for a function $f : \mathcal{X} \rightarrow \mathbb{R}$ where $\mathcal{X} = \prod_{j=1}^d \mathcal{X}_j$. We let $\mathbf{x} = (x_1, \dots, x_d)$ where $x_j \in \mathcal{X}_j$. The ANOVA is defined in terms of a distribution on \mathcal{X} for which the x_j are independent and for which $\mathbb{E}(f(\mathbf{x})^2) < \infty$. The \mathcal{X}_j are ordinarily subsets of \mathbb{R}

but the ANOVA is well defined for more general domains. We let P denote the distribution of \mathbf{x} and P_j denote the distribution of \mathbf{x}_j .

We will use $1:d$ as a short form for $\{1, 2, \dots, d\}$. For sets $u \subseteq 1:d$, their cardinality is $|u|$ and their complement $1:d \setminus u$ is denoted by $-u$. The components x_j for $j \in u$ are collectively denoted by \mathbf{x}_u . We will use hybrid points that merge components from two other points. The point $\mathbf{y} = \mathbf{x}_u : \mathbf{z}_{-u}$ has $y_j = x_j$ for $j \in u$ and $y_j = z_j$ for $j \notin u$. It is typographically convenient to replace singletons $\{j\}$ by j , especially within subscripts.

The ANOVA decomposition writes $f(\mathbf{x}) = \sum_{u \subseteq 1:d} f_u(\mathbf{x})$ where the ‘effect’ f_u depends on \mathbf{x} only through \mathbf{x}_u . The first term is $f_\emptyset(\mathbf{x}) = \mathbb{E}(f(\mathbf{x}))$ and the others are defined recursively via

$$f_u(\mathbf{x}) = \mathbb{E}\left(f(\mathbf{x}) - \sum_{v \subsetneq u} f_v(\mathbf{x}) \mid \mathbf{x}_u\right).$$

The variance component for u is

$$\sigma_u^2 \equiv \text{Var}(f_u(\mathbf{x})) = \begin{cases} \mathbb{E}(f_u(\mathbf{x})^2), & u \neq \emptyset \\ 0, & u = \emptyset. \end{cases}$$

The effects are orthogonal under P and $\sigma^2 = \text{Var}(f(\mathbf{x})) = \sum_u \sigma_u^2$. We will assume that $\sigma^2 > 0$ in order to make some quantities well defined.

Sobol’ indices (Sobol’, 1990, 1993) quantify importance of subsets of input variables on f . His lower and upper indices are

$$\underline{\tau}_u^2 = \sum_{v \subseteq u} \sigma_v^2 \quad \text{and} \quad \bar{\tau}_u^2 = \sum_{v \cap u \neq \emptyset} \sigma_v^2,$$

respectively. These are commonly normalized, with $\underline{\tau}_u^2 / \sigma^2$ known as the closed index and $\bar{\tau}_u^2 / \sigma^2$ is called the total index. Normalized indices are between 0 and 1 giving them interpretations as a proportion of variance explained, similar to R^2 from regression models. The Sobol’ indices $\underline{\tau}_j^2$ and $\bar{\tau}_j^2$ for singletons $\{j\}$ are of special interest. Sobol’ indices satisfy some identities

$$\begin{aligned} \underline{\tau}_u^2 &= \mathbb{E}(f(\mathbf{x})f(\mathbf{x}_u : \mathbf{z}_{-u})) - \mu^2 \\ &= \mathbb{E}(f(\mathbf{x})(f(\mathbf{x}_u : \mathbf{z}_{-u}) - f(\mathbf{z}))) \quad \text{and} \\ \bar{\tau}_u^2 &= \frac{1}{2}\mathbb{E}((f(\mathbf{x}) - f(\mathbf{x}_{-u} : \mathbf{z}_u))^2), \end{aligned}$$

that make it possible to estimate them by Monte Carlo or quasi-Monte Carlo sampling without explicitly computing estimates of any of the effects f_v . The first and third identity are due to Sobol’ (1993). The second was proposed independently by Saltelli (2002) and Mauntz (2002).

The mean dimension of f is

$$\nu(f) = \sum_{u \subseteq 1:d} \frac{|u|\sigma_u^2}{\sigma^2}.$$

It satisfies $1 \leq \nu(f) \leq d$. A low mean dimension indicates that f is dominated by low order ANOVA terms, a favorable property for some numerical problems.

An easy identity from Liu and Owen (2006) shows that $\sum_{u \subseteq 1:d} |u| \sigma_u^2 = \sum_{j=1}^d \bar{\tau}_j^2$. Then the mean dimension of f is

$$\nu(f) \equiv \frac{1}{\sigma^2} \sum_{j=1}^d \bar{\tau}_j^2, \quad \text{for } \bar{\tau}_j^2 = \frac{1}{2} \mathbb{E}((f(\mathbf{x}) - f(\mathbf{x}_{-j}; \mathbf{z}_j))^2).$$

Although the mean dimension combines $2^d - 1$ nonzero variances it can be computed from d Sobol' indices (and the total variance σ^2).

We can get a Monte Carlo estimate of the numerator of $\nu(f)$ by summing estimates of $\bar{\tau}_j^2$ such as

$$\frac{1}{2N} \sum_{i=1}^N (f(\mathbf{x}_i) - f(\mathbf{x}_{i,-j}; \mathbf{z}_{i,j}))^2 \quad (1)$$

for independent random points $\mathbf{x}_i, \mathbf{z}_i \sim P$. There is more than one way to arrange this computation and the choice can make a big difference to the accuracy.

3 Estimation strategies

Equation (1) gives an estimate of $\bar{\tau}_j^2$ evaluating f at pairs of points that differ only in their j 'th coordinate. An estimate for the numerator of $\nu(f)$ sums these estimates. We have found empirically and somewhat surprisingly that different sample methods for computing the numerator $\sum_j \bar{\tau}_j^2$ can have markedly different variances.

A naive implementation uses $2Nd$ function evaluations taking $\mathbf{x}_i, \mathbf{z}_i$ independent for $i = 1, \dots, N$ for each of $j = 1, \dots, d$. In that strategy, the point \mathbf{x}_i in (1) is actually different for each j . Such a naive implementation is wasteful. We could instead use the same \mathbf{x}_i and \mathbf{z}_i for all $j = 1, \dots, d$ in the radial method of Campolongo et al. (2011). This takes $N(d+1)$ evaluations of f . A third strategy is known as 'winding stairs' (Jansen et al., 1994). The data come from a Gibbs sampler, that in its most basic form changes inputs to f one at a time changing indices in this order: $j = 1, \dots, d, 1, \dots, d, \dots, 1, \dots, d$. It uses only $Nd+1$ evaluations of f . These three approaches are illustrated in Figure 1. We will also consider a variant of winding stairs that randomly refreshes after every block of $d+1$ evaluations.

First we compare the naive to the radial strategy. For $\nu = \sum_j \bar{\tau}_j^2 / \sigma^2$ we concentrate on estimation strategies for the numerator

$$\delta = \sigma^2 \nu = \sum_{j=1}^d \bar{\tau}_j^2.$$

This quantity is much more challenging to estimate than the denominator σ^2 , especially for large d , as it involves d^2 covariances.

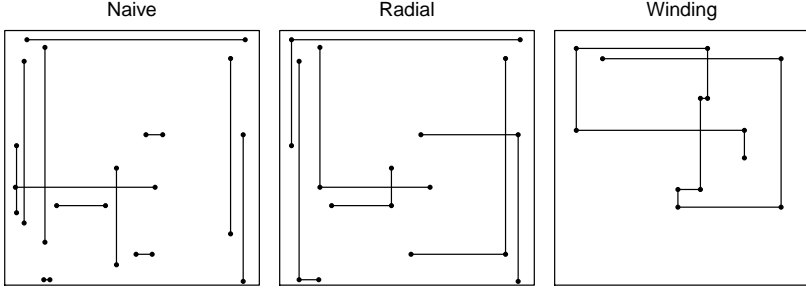


Figure 1: Examples of three input sets to compute $\delta = \sum_{j=1}^d \bar{\tau}_j^2$ when $d = 2$. The naive estimate uses dN pairs of points, N pairs for each of d variables. Each edge connects a pair of points used in the estimate. The radial estimate uses N baseline points and d comparison points for each of them. The winding stairs estimates sequentially changes one input at a time.

The naive sampler takes

$$\hat{\delta} = \sum_{j=1}^d \hat{\tau}_j^2 \quad \text{where} \quad \hat{\tau}_j^2 = \frac{1}{2N} \sum_{i=1}^N (f(\mathbf{x}_i^{(j)}) - f(\mathbf{x}_{i,-j}^{(j)}; \mathbf{z}_{i,j}))^2 \quad (2)$$

with independent $\mathbf{z}_i, \mathbf{x}_i^{(j)} \sim P$ for $i = 1, \dots, N$ and $j = 1, \dots, d$. It takes $N(d+1)$ input vectors and $2Nd$ evaluations of f .

The radial sampler takes

$$\tilde{\delta} = \sum_{j=1}^d \tilde{\tau}_j^2 \quad \text{where} \quad \tilde{\tau}_j^2 = \frac{1}{2N} \sum_{i=1}^N (f(\mathbf{x}_i) - f(\mathbf{x}_{i,-j}; \mathbf{z}_{i,j}))^2, \quad (3)$$

for independent $\mathbf{x}_i, \mathbf{z}_i \sim P$, $i = 1, \dots, N$.

For $f \in L^2(P)$ both $\tilde{\delta}$ and $\hat{\delta}$ converge to $\delta = \nu\sigma^2$ as $N \rightarrow \infty$ by the law of large numbers. To compare accuracy of these estimates we assume also that $f \in L^4(P)$. Then $\mathbb{E}(f(\mathbf{x})^4) < \infty$ and both estimates have variances that are $O(1/N)$.

A first comparison is that

$$\begin{aligned} \text{Var}(\tilde{\delta}) &= \sum_{j=1}^d \text{Var}(\tilde{\tau}_j^2) + 2 \sum_{1 \leq j < k \leq d} \text{Cov}(\tilde{\tau}_j^2, \tilde{\tau}_k^2), \quad \text{while} \\ \text{Var}(\hat{\delta}) &= \sum_{j=1}^d \text{Var}(\hat{\tau}_j^2) + 2 \sum_{1 \leq j < k \leq d} \text{Cov}(\hat{\tau}_j^2, \hat{\tau}_k^2) \\ &= \sum_{j=1}^d \text{Var}(\hat{\tau}_j^2) \end{aligned} \quad (4)$$

by independence of $(\mathbf{x}_i^{(j)}, \mathbf{z}_{i,j})$ from $(\mathbf{x}_i^{(k)}, \mathbf{z}_{i,k})$. What we see from (4) is that while the naive estimate uses about twice as many function evaluations, the radial estimate sums d times as many terms. The off diagonal covariances do not have to be very large for us to have $\text{Var}(\tilde{\delta}) > 2\text{Var}(\hat{\delta})$, in which case $\hat{\delta}$ becomes the more efficient estimate despite using more function evaluations. Intuitively, each time $f(\mathbf{x}_i)$ takes an unusually large or small value it could make a large contribution to all d of $\tilde{\tau}_j^2$ and this can result in $O(d^2)$ positive covariances. We study this effect more precisely below giving additional assumptions under which $\text{Cov}(\tilde{\tau}_j^2, \tilde{\tau}_k^2) > 0$. We also have a numerical counter-example at the end of this section, and so this positive covariance does not hold for all $f \in L^4(P)$.

The winding stairs algorithm starts at $\mathbf{x}_0 \sim P$ and then makes a sequence of single variable changes to generate \mathbf{x}_i for $i > 0$. We let $\ell(i) \in 1:d$ be the index of the component that is changed at step i . The new values are independent samples $z_i \sim P_{\ell(i)}$. That is, for $i > 0$

$$\mathbf{x}_{ij} = \begin{cases} z_i, & j = \ell(i) \\ \mathbf{x}_{i-1,j}, & j \neq \ell(i). \end{cases}$$

We have a special interest in the case where $P = \mathcal{N}(0, I)$ and there each P_j is $\mathcal{N}(0, 1)$.

The indices $\ell(i)$ can be either deterministic or random. We let \mathcal{L} be the entire collection of $\ell(i)$. We assume that the entire collection of z_i are independent of \mathcal{L} . The most simple deterministic update has $\ell(i) = 1 + (i - 1 \bmod d)$ and it cycles through all indices $j \in 1:d$ in order. The simplest random update has $\ell(i) \stackrel{\text{iid}}{\sim} \mathbf{U}(1:d)$. In usual Gibbs sampling it would be better to take $\ell(i) \stackrel{\text{iid}}{\sim} \mathbf{U}(1:d \setminus \{\ell(i-1)\})$ for $i \geq 2$. Here because we are accumulating squared differences it is not very harmful to have $\ell(i) = \ell(i-1)$. The vector \mathbf{x}_i contains d independently sampled Gaussian random variables. Which ones those are, depends on \mathcal{L} . Because $\mathbf{x} \sim \mathcal{N}(0, I)$ conditionally on \mathcal{L} it also has that distribution unconditionally.

Letting e_j be the j 'th unit vector in \mathbb{R}^d we can write

$$\mathbf{x}_i = \mathbf{x}_{i-1} + (z_i - x_{i-1, \ell(i)}) e_{\ell(i)}.$$

If $\ell(i) \sim \mathbf{U}(1:d)$, then the distribution of \mathbf{x}_i given \mathbf{x}_{i-1} is a mixture of d different Gaussian distributions, one for each value of $\ell(i)$. As a result $\mathbf{y}_i = (\mathbf{x}_i^\top, \mathbf{x}_{i-1}^\top)^\top$ does not then have a multivariate Gaussian distribution and is harder to study. For this reason, we focus on the deterministic update.

In the deterministic update we find that any finite set of \mathbf{x}_i or \mathbf{y}_i has a multivariate Gaussian distribution. We also know that \mathbf{x}_i and \mathbf{x}_{i+k} are independent for $k \geq d$ because after k steps all components of \mathbf{x}_i have been replaced by new z_i values. It remains to consider the correlations among a block of $d+1$ consecutive vectors. Those depend on the pattern of shared components within

different observations as illustrated in the following diagram:

$$\begin{array}{cccccc}
\mathbf{x}_d & \mathbf{x}_{d+1} & \mathbf{x}_{d+2} & \cdots & \mathbf{x}_{2d-1} & \mathbf{x}_{2d} \\
\parallel & \parallel & \parallel & & \parallel & \parallel \\
\begin{pmatrix} z_1 \\ z_2 \\ \vdots \\ z_{d-1} \\ z_d \end{pmatrix} & \begin{pmatrix} z_{d+1} \\ z_2 \\ \vdots \\ z_{d-1} \\ z_d \end{pmatrix} & \begin{pmatrix} z_{d+1} \\ z_{d+2} \\ \vdots \\ z_{d-1} \\ z_d \end{pmatrix} & \cdots & \begin{pmatrix} z_{d+1} \\ z_{d+2} \\ \vdots \\ z_{2d-1} \\ z_d \end{pmatrix} & \begin{pmatrix} z_{d+1} \\ z_{d+2} \\ \vdots \\ z_{2d-1} \\ z_{2d} \end{pmatrix}.
\end{array} \quad (5)$$

For $i \geq d$ and $j = 1, \dots, d$ we can write

$$\mathbf{x}_{i,j} = z_{r(i,j)} \quad \text{where} \quad r(i,j) = d \left\lfloor \frac{i-j}{d} \right\rfloor + j. \quad (6)$$

It is convenient to use (6) for all $i \geq 0$ which is equivalent to initializing the sampler at $\mathbf{x}_0 = (z_{-(d-1)}, z_{-(d-2)}, \dots, z_{-1}, z_0)^\top$. Equation (6) holds for any independent $z_i \sim P_{\ell(i)}$ and does not depend on our choice of $P_j = \mathcal{N}(0, 1)$.

The winding stairs estimate of δ is

$$\check{\delta} = \sum_{j=1}^d \check{\tau}_j^2 \quad \text{for} \quad \check{\tau}_j^2 = \frac{1}{2N} \sum_{i=1}^N \Delta_{d(i-1)+j}^2, \quad (7)$$

where $\Delta_r = f(\mathbf{x}_r) - f(\mathbf{x}_{r-1})$. We will see that the covariances of $\check{\tau}_j^2$ and $\check{\tau}_k^2$ depend on the pattern of common components among the \mathbf{x}_i . In our special case functions certain kurtoses have an impact on the variance of winding stairs estimates.

A useful variant of winding stairs simply makes N independent replicates of the $d+1$ vectors shown in (5). That raises the number of function evaluations from $Nd+1$ to $N(d+1)$. It uses N independent Markov chains of length $d+1$. For large d the increased computation is negligible. For $d=2$ this disjoint winding stairs method is the same as the radial method. In original winding stairs, each squared difference $\Delta_i^2 = (f(\mathbf{x}_i) - f(\mathbf{x}_{i-1}))^2$ can be correlated with up to $2(d-1)$ other squared differences. In disjoint winding stairs, it can only be correlated with $d-1$ other squared differences. We denote the resulting estimate by $\check{\delta}$ which is a sum of $\check{\tau}_j^2$.

In section 4 we present some multiplicative functions where the naive estimator of δ has much less than half of the variance of the radial estimator. To complete this section we exhibit a numerical example where the naive estimator has increased variance which must mean that the correlations induced by the radial and winding estimators are at least slightly negative. The integrand is simply $f(\mathbf{x}) = \|\mathbf{x}\|_2$ for $\mathbf{x} \sim \mathcal{N}(0, I)$ in d dimensions. Figure 2 shows results. We used $N = 10^6$ evaluations to show that (truncated) winding stairs and radial sampling both have smaller variance than the naive algorithm for estimating δ . We also see extremely small mean dimensions for $f(\mathbf{x})$ that decrease as d increases. It relates to some work in progress studying mean dimension of radial

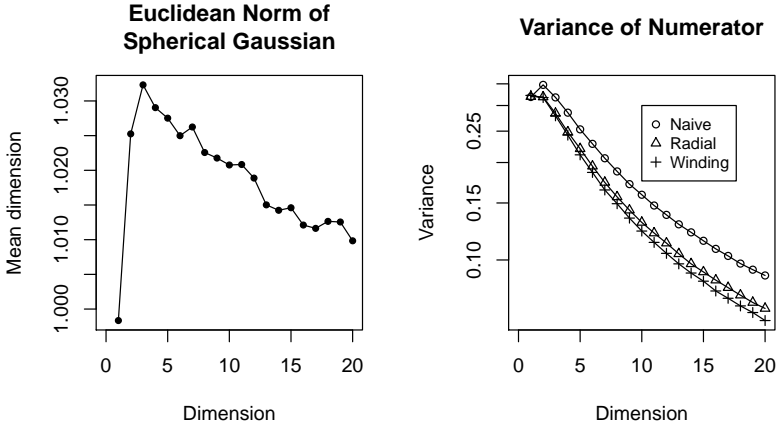


Figure 2: The left panel shows low and mostly decreasing estimates of $\nu(f)$ versus dimension for $f(\mathbf{x}) = \|\mathbf{x}\|_2$ when $\mathbf{x} \sim \mathcal{N}(0, I)$. The right panel shows variances of estimates of δ for this function.

basis functions as a counterpart to Hoyt and Owen (2020) on mean dimension of ridge functions. The visible noise in that figure stems from the mean dimensions all being so very close to 1 that the vertical range is quite small. The estimate for $d = 1$ is roughly 0.9983 where the true value must be 1.

4 Additive and multiplicative functions

The variances of quadratic functions of the $f(\mathbf{x}_i)$ values such as $\hat{\delta}$, $\tilde{\delta}$ and $\check{\delta}$, involve fourth moments of the original function. Whereas 2^d variance components are sufficient to define Sobol' indices and numerous generalizations, fourth moments do not simplify nearly as much from orthogonality and involve considerably more quantities. While distinct pairs of ANOVA effects are orthogonal, we find for non-empty $u, v, w \subset 1:d$ that

$$\mathbb{E}(f_u(\mathbf{x})f_v(\mathbf{x})f_w(\mathbf{x}))$$

does not in general vanish when $u \subset v \cup w$, $v \subset u \cup w$ and $w \subset u \cup v$ all hold. This ‘chaining phenomenon’ is worse for products of four effects: the number of non-vanishing combinations rises even more quickly with d . The chaining problem also comes up if we expand f in an orthonormal basis for $L^2(P)$ and then look at fourth moments.

In this section we investigate some special functional forms. The first is an additive model

$$f_A(\mathbf{x}) = \mu + \sum_{j=1}^d g_j(x_j) \quad (8)$$

where $\mathbb{E}(g_j(x_j)) = 0$. An additive model with finite variance has mean dimension $\nu(f_A) = 1$. It represents one extreme in terms of mean dimension. The second function we consider is a product model

$$f_P(\mathbf{x}) = \prod_{j=1}^d g_j(x_j) \quad (9)$$

where $\mathbb{E}(g_j(x_j)) = \mu_j$ and $\text{Var}(g_j(x_j)) = \sigma_j^2$. Product functions are frequently used as test functions. For instance, Sobol's g -function (Saltelli and Sobol', 1995) is the product $\prod_{j=1}^d (|4x_j - 2| + a_j)/(1 + a_j)$ in which later authors make various choices for the constants a_j .

If all $\mu_j = 0$ then $\nu(f_P) = d$. In general, the mean dimension of a product function is

$$\nu(f_P) = \frac{\sum_{j=1}^d \sigma_j^2 / (\mu_j^2 + \sigma_j^2)}{1 - \prod_{j=1}^d \mu_j^2 / (\mu_j^2 + \sigma_j^2)}.$$

See Owen (2003).

We will use Lemma 1 below to compare the variances of our mean dimension estimators. We will need some additional moments. For a random variable Y , define the skewness $\gamma = \mathbb{E}((Y - \mu)^3)/\sigma^3$ and the kurtosis $\kappa = \mathbb{E}((Y - \mu)^4)/\sigma^4 - 3$. Gaussian random variables have $\gamma = \kappa = 0$.

Lemma 1. *Let Y_1, Y_2, Y_3, Y_4 be independent identically distributed random variables with variance σ^2 and kurtosis κ . Then*

$$\begin{aligned} \mathbb{E}((Y_1 - Y_2)^4) &= (12 + 2\kappa)\sigma^4 \\ \text{Var}((Y_1 - Y_2)^2) &= (8 + 2\kappa)\sigma^4 \\ \mathbb{E}((Y_1 - Y_2)^2(Y_3 - Y_4)^2) &= 4\sigma^4 \\ \mathbb{E}((Y_1 - Y_2)^2(Y_1 - Y_3)^2) &= (6 + \kappa)\sigma^4. \end{aligned}$$

Proof. These follow directly from independence of the Y_j and the definitions of variance and kurtosis. \square

Theorem 1. *For the additive function f_A of (8),*

$$\text{Var}(\check{\delta}) = \text{Var}(\hat{\delta}) = \text{Var}(\ddot{\delta}) = \frac{1}{N} \sum_{j=1}^d \left(2 + \frac{\kappa_j}{2}\right) \sigma_j^4 \quad (10)$$

and

$$\text{Var}(\check{\delta}) = \text{Var}(\ddot{\delta}) + \frac{N-1}{2N^2} \sum_{j=1}^d (\kappa_j + 2) \sigma_j^4. \quad (11)$$

Proof. The winding stairs results for $\check{\delta}$ and $\ddot{\delta}$ quoted above are proved in Theorem 3 of the Appendix. For the naive estimate, $\hat{\tau}_j^2$ is independent of $\hat{\tau}_k^2$ when $j \neq k$ as remarked upon at (4). For an additive function

$$f_A(\mathbf{x}_i) - f_A(\mathbf{x}_{i,-j}; \mathbf{z}_{i,j}) = g_j(x_{ij}) - g_j(z_{ij})$$

is independent of $g_k(x_{ik}) - g_k(z_{ik})$ for $j \neq k$ and so the radial estimate has the same independence property as the naive estimate. Therefore

$$\text{Var}(\widehat{\tau}_j^2) = \text{Var}(\widetilde{\tau}_j^2) = \frac{1}{4N} \text{Var}((g_j(x_{1j}) - g_j(z_{1j}))^2)$$

and using Lemma 1, $\text{Var}((g_j(x_{1j}) - g_j(z_{1j}))^2) = (8 + 2\kappa_j)\sigma_j^4$. \square

If $f(\mathbf{x})$ is additive, then Theorem 1 shows that the radial method is better than the naive one. They have the same variance but the naive method uses roughly twice as many function evaluations. If the function is nearly additive, then it is reasonable to expect the variances to be nearly equal and the radial method to be superior. Because $\kappa_j \geq 2$ always holds the theorem shows an advantage to disjoint winding stairs over plain winding stairs.

We turn next to functions of product form. To simplify some expressions for winding stairs we adopt the conventions that for $1 \leq j < k \leq d$ and quantities q_ℓ , $\prod_{\ell \in (j, k)} q_\ell$ means $\prod_{\ell=j+1}^{k-1} q_\ell$, $\prod_{\ell \notin [j, k]} q_\ell$ means $\prod_{\ell=1}^{j-1} q_\ell \times \prod_{\ell=k+1}^d q_\ell$ and products over empty index sets equal one.

Theorem 2. *For the product function f_P of (9),*

$$\text{Var}(\hat{\delta}) = \frac{1}{N} \sum_{j=1}^d \sigma_j^4 \left(\left(3 + \frac{\kappa_j}{2} \right) \prod_{\ell \neq j} \mu_{4\ell} - \prod_{\ell \neq j} \mu_{2\ell}^2 \right) \quad \text{and} \quad (12)$$

$$\text{Var}(\tilde{\delta}) = \text{Var}(\hat{\delta}) + \frac{2}{N} \sum_{j < k} \left(\frac{\eta_j \eta_k}{4} - \sigma_j^2 \sigma_k^2 \mu_{2j} \mu_{2k} \right) \prod_{\ell \notin \{j, k\}} \mu_{4\ell}, \quad (13)$$

where $\eta_j = \mathbb{E}(g_j(x_j)^2(g_j(x_j) - g_j(z_j))^2) = \mu_{4j} - 2\mu_j \mu_{3j} + \mu_{2j}^2$, for independent $x_j, z_j \sim P_j$. The winding stairs estimates satisfy

$$\text{Var}(\ddot{\delta}) = \text{Var}(\hat{\delta}) + \frac{2}{N} \sum_{j < k} \left(\frac{\eta_j \eta_k}{4} \prod_{\ell \in (j, k)} \mu_{2\ell}^2 \prod_{\ell \notin [j, k]} \mu_{4\ell} - \sigma_j^2 \sigma_k^2 \mu_{2j} \mu_{2k} \prod_{\ell \notin [j, k]} \mu_{2\ell}^2 \right) \quad (14)$$

and

$$\text{Var}(\check{\delta}) = \text{Var}(\ddot{\delta}) + \frac{2}{N} \sum_{j < k} \left(\frac{\eta_j \eta_k}{4} \prod_{\ell \notin [j, k]} \mu_{4\ell} - \sigma_j^2 \sigma_k^2 \prod_{\ell \notin [j, k]} \mu_{2\ell}^2 \right) \prod_{\ell \in (j, k)} \mu_{2\ell}^2. \quad (15)$$

Proof. The winding stairs results are from Theorem 4 in the Appendix. Next we turn to the naive estimator. For $\mathbf{x}, \mathbf{z} \sim P$ independently, define $\Delta_j = \Delta_j(\mathbf{x}, \mathbf{z}) \equiv f_P(\mathbf{x}) - f_P(\mathbf{x}_{-j}; \mathbf{z}_j)$. Now

$$\Delta_j = (g_j(x_j) - g_j(z_j)) \times \prod_{\ell \neq j} g_\ell(x_\ell)$$

and so $\mathbb{E}(\Delta_j^2) = 2\sigma_j^2 \times \prod_{\ell \neq j} \mu_{2\ell}$ and $\mathbb{E}(\Delta_j^4) = (12 + 2\kappa_j)\sigma_j^4 \times \prod_{\ell \neq j} \mu_{4j}$, from Lemma 1. Therefore

$$\text{Var}(\Delta_j^2) = (12 + 2\kappa_j)\sigma_j^4 \times \prod_{\ell \neq j} \mu_{4j} - 4\sigma_j^4 \times \prod_{\ell \neq j} \mu_{2\ell}^2.$$

establishing (12).

In the radial estimate, Δ_j is as above and $\Delta_k = (g_k(x_k) - g_k(z_k)) \times \prod_{\ell \neq k} g_\ell(x_\ell)$. In this case however the same point \mathbf{x} is used in both Δ_j and Δ_k so $\mathbb{E}(\Delta_j^2 \Delta_k^2)$ equals

$$\begin{aligned} & \mathbb{E} \left(g_j(x_j)^2 g_k(x_k)^2 (g_j(x_j) - g_j(z_j))^2 (g_k(x_k) - g_k(z_k))^2 \prod_{\ell \notin \{j, k\}} g_\ell(x_\ell)^4 \right) \\ &= \eta_j \eta_k \prod_{\ell \notin \{j, k\}} \mu_{4\ell}. \end{aligned}$$

Then $\text{Cov}(\Delta_j^2, \Delta_k^2) = (\eta_j \eta_k - 4\sigma_j^2 \sigma_k^2 \mu_{2j} \mu_{2k}) \prod_{\ell \notin \{j, k\}} \mu_{4\ell}$, establishing (13). \square

We comment below on interpretations of the winding stairs quantities. First we compare naive to radial sampling.

As an illustration, suppose that $g_j(x_j) \sim \mathcal{N}(0, 1)$ for $j = 1, \dots, d$. Then

$$\text{Var}(\hat{\delta}) = \frac{1}{N} \sum_{j=1}^d (3^d - 1) = \frac{(3^d - 1)d}{N}$$

and since this example has $\eta_j = 4$,

$$\text{Var}(\tilde{\delta}) = \frac{d(3^d - 1)}{N} + \frac{2}{N} \sum_{j < k} \left(\frac{16}{4} - 1 \right) 3^{d-2} = \frac{d(3^d - 1)}{N} + \frac{2d(d-1)3^{d-1}}{N}.$$

For large d the radial method has variance about $2d/3$ times as large as the naive method. Accounting for the reduced sample size of the radial method it has efficiency approximately $3/d$ compared to the naive method, for this function.

A product of mean zero functions has mean dimension d making it an exceptionally hard case. More generally, if $\eta_j/2 - \sigma_j^2 \mu_{2j} \geq \epsilon > 0$ for $j \in 1:d$, then $\text{Var}(\hat{\delta}) = O(d/N)$ while $\text{Var}(\tilde{\delta})$ is larger than a multiple of d^2/N .

Corollary 1. *For the product function f_P of (9), suppose that $\kappa_j \geq -5/16$ for $j = 1, \dots, d$. Then $\text{Cov}(\tilde{\tau}_j^2, \tilde{\tau}_k^2) \geq 0$ for $1 \leq j < k \leq d$, and so $\text{Var}(\tilde{\delta}) \geq \text{Var}(\hat{\delta})$.*

Proof. It suffices to show that $\eta_j > 2\sigma_j^2 \mu_{2j}$ for $j = 1, \dots, d$. Let $Y = g_j(x_j)$ for $x_j \sim P_j$ have mean μ , uncentered moments μ_{2y} , μ_{3y} and μ_{4y} of orders 2, 3 and 4, respectively, variance σ^2 , skewness γ , and kurtosis κ . Now let $\eta = \mu_{4y} - 2\mu\mu_{3y} + \mu_{2y}^2$. This simplifies to

$$\eta = (\kappa + 2)\sigma^4 + 2\mu\sigma^3\gamma + 2\mu^2\sigma^2 + \sigma^4$$

and so

$$\eta - 2\sigma^2 \mu_{2y} = (\kappa + 2)\sigma^4 + 2\mu\sigma^3\gamma + \mu^2\sigma^2.$$

If $\sigma = 0$ then $\eta - 2\sigma^2 \mu_{2y} = 0$ and so we suppose that $\sigma > 0$. Replacing Y by Y/σ does not change the sign of $\eta - 2\sigma^2 \mu_{2y}$. It becomes $\kappa + 2 + 2\mu_*\gamma + \mu_*^4$

for $\mu_* = \mu/\sigma$. If γ and μ_* have equal signs, then $\kappa + 2 + 2\mu_*\gamma + \mu_*^4 \geq 0$, so we consider the case where they have opposite signs. Without loss of generality we take $\gamma < 0 < \mu_*$. An inequality of Rohatgi and Székely (1989) shows that $|\gamma| \leq \sqrt{\kappa + 2}$ and so

$$\kappa + 2 + 2\mu_*\gamma + \mu_*^4 \geq \theta^2 - 2\mu_*\theta + \mu_*^4 \quad (16)$$

for $\theta = \sqrt{\kappa + 2}$. Equation (16) is minimized over $\mu_* \geq 0$ at $\mu_* = (\theta/2)^{1/3}$ and so $\kappa + 2 + 2\mu_*\gamma + \mu_*^4 \geq \theta^2 + (2^{-4/3} - 2^{2/3})\theta^{4/3}$. One last variable change to $\theta = (2\lambda)^3$ gives

$$\kappa + 2 + 2\mu_*\gamma + \mu_*^4 \geq \lambda^4(4\lambda^2 - 3).$$

This is nonnegative for $\lambda \geq (3/4)^{1/2}$, equivalently $\theta \geq 2(3/4)^{3/2}$ and finally for $\kappa \geq -5/16$. \square

From the above discussion we can see that large kurtoses and hence large values of $\mu_{4j} = \mathbb{E}(g_j(x_j)^4)$ create difficulties. In this light we can compare winding stairs to the radial sampler. The covariances in the radial sampler involve a product of $d - 2$ of the μ_{4j} . The winding stairs estimates involve products of fewer of those quantities. For disjoint winding stairs the j, k -covariance include a product of only $d - k + j - 1$ of them. The values $\mu_{4\ell}$ for ℓ nearest to 1 and d appear the most often and so the ordering of the variables makes a difference. For regular winding stairs some additional fourth moments appear in a second term.

5 Example: MNIST classification

In this section, we investigate the mean dimension of a neural network classifier that predicts a digit in $\{0, 1, \dots, 9\}$ based on an image of 784 pixels. We compare algorithms for finding mean dimension, investigate some mean dimensions, and then plot some images of Sobol' indices.

The MNIST data set from <http://yann.lecun.com/exdb/mnist/> is a very standard benchmark problem for neural networks. It consists of 70,000 images of hand written digits that were size-normalized and centered within 28×28 pixel gray scale images. We normalize the image values to the unit interval, $[0, 1]$. The prediction problem is to identify which of the ten digits '0', '1', ..., '9' is in one of the images based on $28^2 = 784$ pixel values. We are interested in the mean dimension of a fitted prediction model.

The model we used is a convolutional neural network fit via tensorflow (Abadi et al., 2016). The architecture applied the following steps to the input pixels in order:

- 1) a convolutional layer (with 28 kernels, each of size 3x3),
- 2) a max pooling layer (over 2x2 blocks),
- 3) a flattening layer,
- 4) a fully connected layer with 128 output neurons (ReLU activation),
- 5) a dropout layer (node values were set to 0 with probability 0.2), and

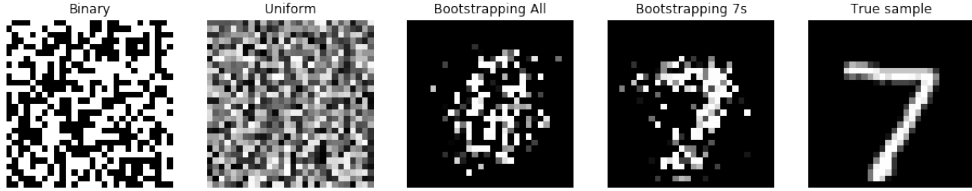


Figure 3: From left to right: draws from $\mathbf{U}\{0, 1\}^{28 \times 28}$, $\mathbf{U}[0, 1]^{28 \times 28}$, margins of all images, margins of all 7s, an example 7.

6) a final fully connected layer with 10 output neurons (softmax activation). This model is from Yalcin (2018) who also defines those terms. The network was trained using 10 epochs of ADAM optimization, also described in Yalcin (2018), on 60,000 training images. For our purposes, it is enough to know that it is a complicated black box function of 784 inputs. The accuracy on 10,000 held out images was 98.5%. This is not necessarily the best accuracy attained for this problem, but we consider it good enough to make the prediction function worth investigating.

There are $2^{784} - 1 > 10^{236}$ nontrivial sets of pixels, each making their own contribution to the prediction functions, but the mean dimension can be estimated by summing only 784 Sobol' indices.

We view the neural network's prediction as a function on 784 input variables \mathbf{x} . For data (\mathbf{x}, Y) where $Y \in \{0, 1, \dots, 9\}$ is the true digit of the image, the estimated probability that $Y = y$ is given by

$$f_y(\mathbf{x}) = \frac{\exp(g_y(\mathbf{x}))}{\sum_{\ell=0}^9 \exp(g_\ell(\mathbf{x}))}.$$

for functions g_y , $0 \leq y \leq 9$. This last step, called the softmax layer, exponentiates and normalizes functions g_y that implement the prior layers. We study the mean dimension of g_0, \dots, g_9 as well as the mean dimensions of f_0, \dots, f_9 . Studying the complexity of predictions via the inputs to softmax has been done earlier Yosinski et al. (2015).

To compute mean dimension we need to have a model for \mathbf{x} with 784 independent components. Real images are only on or near a very small manifold within \mathbb{R}^{784} . We considered several distributions P_j for the value of pixel j : $\mathbf{U}\{0, 1\}$ (salt and pepper) $\mathbf{U}[0, 1]$ (random gray), independent resampling from per pixel histograms of all images, and independent resampling per pixel just from images with a given value of $y \in \{0, 1, \dots, 9\}$. The histogram of values for pixel j from those images is denoted by $h_y(j)$ with h_y representing all 784 of them. Figure 3 shows some sample draws along with one real image. We think that resampling pixels from images given y is the most relevant of these methods, though ways to get around the independence assumption would be valuable. We nonetheless include the other samplers in our computations.

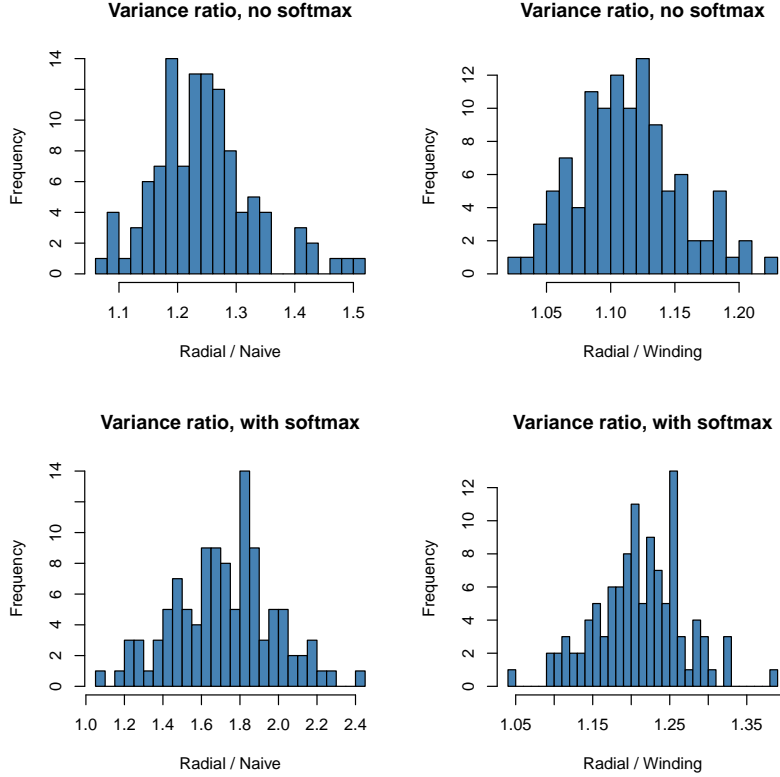


Figure 4: The upper left histogram shows $\text{Var}(\tilde{\delta})/\text{Var}(\hat{\delta})$ for functions g_y that exclude softmax. The upper right histogram shows $\text{Var}(\tilde{\delta})/\text{Var}(\ddot{\delta})$. The bottom two show the same ratios for functions f_y that include softmax. The histograms include all 10 values of output y , and all 10 y -specific input histograms and the pooled input histogram.

Our main interest is in comparing the variance of estimates of δ . We compared the naive method $\hat{\delta}$, the radial method $\tilde{\delta}$ and truncated winding stairs $\ddot{\delta}$. For $\ddot{\delta}$ our winding stairs algorithm changed pixels in raster order, left to right within rows, taking rows of the image from top to bottom. We omit $\ddot{\delta}$ because we think there is no benefit from its more complicated model and additional correlations. Our variance comparisons are based on $N = 100,000$ samples.

Figure 4 shows the results for all 10 output values y , all 11 input histogram distributions, with separate plots for functions f_y that include softmax and g_y that exclude it. The radial method always had greater variance than the naive method. For functions g_y it never had as much as twice the variance of the naive method, and so the radial method proves better for g_y . For f_y there were some exceptions where the naive method is more efficient. In all of our comparisons

Sampler	0	1	2	3	4	5	6	7	8	9
binary	11.07	936.04	10.43	9.92	18.69	10.22	13.27	13.37	8.67	16.54
uniform	6.92	4,108.99	7.28	6.60	9.90	7.03	6.92	8.03	5.61	9.48
combined	8.77	4.68	4.06	3.95	4.56	5.11	7.62	4.62	3.43	7.39
0	3.52	6.81	3.48	7.20	6.56	5.78	7.54	4.67	4.04	9.08
1	36.12	2.88	6.00	3.43	7.75	3.76	8.74	7.60	2.83	5.58
2	10.03	3.86	3.68	4.70	8.23	12.27	12.57	7.20	4.31	17.23
3	23.20	4.69	5.95	4.10	6.96	6.72	13.63	7.10	4.42	9.00
4	7.42	8.39	7.59	9.96	3.81	7.63	8.57	5.35	3.86	6.82
5	8.12	4.77	5.72	4.82	5.60	3.48	7.61	7.28	3.54	7.87
6	9.22	5.65	4.36	6.52	4.31	6.67	3.57	6.43	4.28	11.99
7	8.57	5.85	4.42	4.09	4.66	5.09	3.59	3.59	4.29	5.58
8	19.58	6.06	4.54	4.77	8.21	6.28	13.15	6.72	4.20	10.11
9	7.47	7.00	5.25	4.96	3.15	4.52	7.34	3.74	2.92	3.48

Table 1: Estimated mean dimension of functions f_y using softmax.

the winding stairs method had lower variance than the radial method, and so for these functions, (truncated) winding stairs is clearly the best choice.

Figure 4 is a summary of 660 different variance estimates. We inspected the variances and found two more things worth mentioning but not presenting. The variances were all far smaller using softmax than not, which is not surprising since softmax compresses the range of f_y to be within $[0, 1]$ which will greatly affect the differences that go into estimates of δ . The variances did not greatly depend on the input distribution. While there were some statistically significant differences, which is almost inevitable for such large N , the main practical difference was that variances tended to be much smaller when sampling from h_1 . We believe that this is because images for $y = 1$ have much less total illumination than the others.

While our main purpose is to compare estimation strategies for mean dimension, the mean dimensions for this problem are themselves of interest. Table 1 shows mean dimensions for functions f_y that include softmax as estimated via winding stairs. For this we used $N = 10^6$ when resampling from images h_0, \dots, h_9 and $N = 2 \times 10^6$ otherwise. The first thing to note is an impossible estimate of $\nu(f_1)$ for binary and uniform sampling. The true $\nu(f_1)$ cannot be larger than 784. The function f_1 has tiny variance under those distributions and recall that $\nu = \delta/\sigma^2$. Next we see that moving from binary to uniform to the combined histogram generally lowers the mean dimension. Third, for the y -specific histograms h_y we typically see smaller mean dimensions for f_y with the same y that was used in sampling. That is, the diagonal of the lower block tends to have smaller values.

Table 2 shows mean dimensions for functions g_y that exclude softmax as estimated via winding stairs. They are all in the range from 1.35 to 1.92. We found no particular problem with the function g_1 like we saw for f_1 . While the functions g_y that are sent into softmax were obtained by a very complicated

Sampler	0	1	2	3	4	5	6	7	8	9
binary	1.66	1.76	1.74	1.72	1.73	1.79	1.75	1.69	1.74	1.79
uniform	1.65	1.62	1.66	1.66	1.67	1.71	1.71	1.61	1.68	1.70
combined	1.79	1.77	1.70	1.73	1.73	1.90	1.88	1.78	1.90	1.89
0	1.92	1.65	1.68	1.69	1.65	1.80	1.86	1.56	1.68	1.81
1	1.48	1.56	1.35	1.61	1.62	1.57	1.49	1.42	1.56	1.50
2	1.55	1.66	1.62	1.74	1.57	1.72	1.67	1.61	1.78	1.59
3	1.56	1.65	1.59	1.58	1.63	1.85	1.59	1.64	1.67	1.66
4	1.87	1.62	1.61	1.55	1.70	1.75	1.76	1.66	1.57	1.78
5	1.71	1.60	1.59	1.63	1.72	1.78	1.74	1.62	1.76	1.90
6	1.65	1.60	1.60	1.66	1.68	1.70	1.65	1.60	1.54	1.63
7	1.73	1.59	1.61	1.63	1.60	1.62	1.65	1.57	1.59	1.63
8	1.73	1.65	1.60	1.64	1.66	1.78	1.75	1.64	1.84	1.75
9	1.86	1.68	1.61	1.63	1.73	1.80	1.86	1.67	1.69	1.82

Table 2: Estimated mean dimension of functions g_y without softmax.

process, they do not make much use of very high order interactions. There must be a significantly large component of additive functions and two factor interactions within them. There may be a small number of large high order interactions but they do not dominate any of the functions f_y under any of the sampling distributions we use. The softmax function begins by exponentiating f_y which we can think of as changing a function with a lot of additive structure into one with a lot of multiplicative structure. Multiplicative functions can have quite high mean dimension.

The measured mean dimensions of g_y are pretty stable as the sampling distribution changes. While the manifold of relevant images is likely to be quite small, it is reassuring that 13 different independent data distributions give largely consistent and small mean dimensions.

Figure 5 shows some Sobol' indices of f_y and g_y for $y \in \{0, 1, \dots, 9\}$ when sampling from h_0 . In each set of 10 images, the gray scale goes from black for 0 to white for the largest intensity in any of those 10 images. As a consequence some of the images are almost entirely black.

The lower indices $\underline{\tau}_j^2$ depict the importance of inputs one at a time. This is similar to what one gets from a gradient, see for instance Grad-cam (Selvaraju et al., 2017), except that $\underline{\tau}_j^2$ is global over the whole range of the input instead of local like a gradient. Upper indices $\underline{\tau}_j^2$ depict the importance of each pixel combining all of the interactions to which it contributes, not just its main effect.

For the influence on f_0 when sampling from h_0 , the difference between $\underline{\tau}_j^2$ and $\bar{\tau}_j^2$ is in that bright spot just left of the center of the image. That is the region of pixels involved in the most interactions. It appears to be involved in distinguishing 0s from 2s and 8s because that region is also bright for functions f_2 and f_8 . Without softmax that bright spot for $\underline{\tau}_j^2$ is lessened and so we see that much though not all of its interaction importance was introduced by the softmax layer. For g_5 when sampling from h_0 we see that a region just Northeast

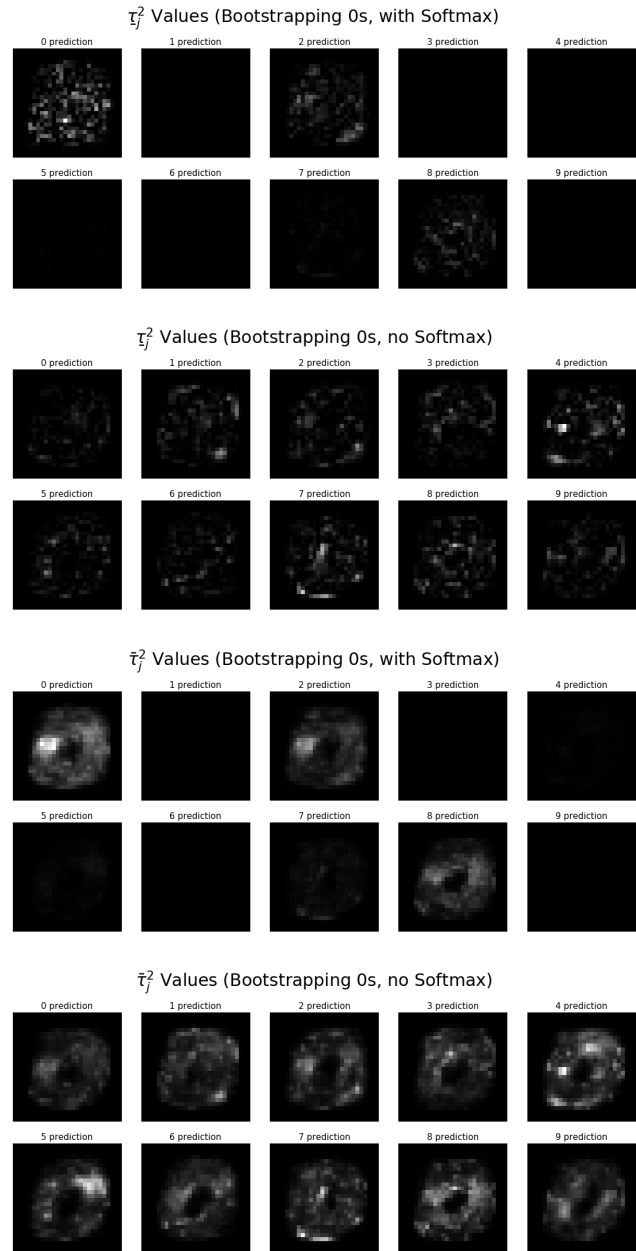


Figure 5: From top to bottom: maps of $\tau_j^2(f_y)$, $\tau_j^2(g_y)$, $\bar{\tau}_j^2(f_y)$ and $\bar{\tau}_j^2(g_y)$ versus pixels j when sampling from h_0 .

of the center of the image has the most involvement in interactions as measured by $\underline{\tau}_j^2$.

6 Discussion

We have found that the strategy under which differences of function values are collected can make a big difference to the statistical efficiency of estimates of mean dimension. Computational efficiency in reusing function values can increase some correlations enough to more than offset that advantage. Whether this happens depends on the function involved. We have seen examples where high kurtoses make the problem worse.

Our interest in mean dimension leads us to consider sums of $\bar{\tau}_j^2$. In other uncertainty quantification problems we are interested in comparing and ranking $\bar{\tau}_j^2$. For a quantity like $\hat{\tau}_j^2 - \hat{\tau}_k^2$ we actually prefer a large positive value for $\text{Cov}(\hat{\tau}_j^2, \hat{\tau}_k^2)$. In this case, the disadvantages we described for the radial method become a strength. Correlation effects are more critical for mean dimension than for these differences of Sobol' indices, because mean dimension is affected by $O(d^2)$ covariances, not just one.

The radial strategy and the disjoint winding stairs strategy can both be represented in terms of a tree structure connecting $d+1$ function values. There is a one to one correspondence between the d edges in that tree and the components of \mathbf{x} getting changed. There is no particular reason to think that either of these strategies is the optimal graph structure or even the optimal tree.

We have studied the accuracy of mean dimension estimates as if the sampling were done by plain Monte Carlo (MC). When P is the uniform distribution on $[0, 1]^d$ then we can instead use randomized quasi-Monte Carlo (RQMC) sampling, surveyed in L'Ecuyer and Lemieux (2002). The naive method can be implemented using N points in $[0, 1]^{d+1}$ for each of $j = 1, \dots, d$. The first column of the j 'th input matrix could contain \mathbf{z}_{ij} for $i = 1, \dots, N$ while the remaining d columns would have $\mathbf{x}_i^{(j)} \in [0, 1]^d$. The $d+1$ 'st point contains the values $\mathbf{x}_{i,j}$. The radial method can be implemented with N points in $[0, 1]^{2d}$ with the first d columns providing \mathbf{x}_i and the second d columns providing \mathbf{z}_i , both for $i = 1, \dots, N$. Disjoint winding stairs, similarly requires N points in $[0, 1]^{2d}$. For RQMC sampling by scrambled nets, the resulting variance is $o(1/N)$. A reasonable choice is to use RQMC in whichever method one thinks would have the smallest MC variance. The rank ordering of RQMC variances could however be different from that of MC and it could even change with N , so results on MC provide only a suggestion of which method would be best for RQMC.

A QMC approach to plain winding stairs would require QMC methods designed specifically for MCMC sampling. See for instance, one based on completely uniformly distributed sequences described in Owen and Tribble (2005).

We have used a neural network black box function to illustrate our computations. It is yet another example of an extremely complicated function that nonetheless is dominated by low order interactions. In problems like this where

the input images had a common registration an individual pixel has some persistent meaning between images and then visualizations of $\underline{\tau}_j^2$ can be informative. Many neural network problems are applied to data that have not been so carefully registered as the MNIST data. For those problems the link from predictions back to inputs may need to be explored in a different way.

Acknowledgments

This work was supported by a grant from Hitachi Limited and by the US National Science Foundation under grant IIS-1837931. We thank Masayoshi Mase of Hitachi for helpful discussions about variable importance and explainable AI.

References

Abadi, M., Barham, P., Chen, J., Chen, Z., Davis, A., Dean, J., Devin, M., Ghemawat, S., Irving, G., Isard, M., Kudlur, M., Levenberg, J., Monga, R., Moore, S., Murray, D. G., Steiner, B., Tucker, P., Vasudevan, V., Warden, P., Wicke, M., Yu, Y., and Zheng, X. (2016). Tensorflow: A system for large-scale machine learning. In *12th USENIX Symposium on Operating Systems Design and Implementation (OSDI '16)*, pages 265–283.

Campolongo, F., Saltelli, A., and Cariboni, J. (2011). From screening to quantitative sensitivity analysis. a unified approach. *Computer Physics Communications*, 182(4):978–988.

Hoyt, C. and Owen, A. B. (2020). Mean dimension of ridge functions. *SIAM Journal on Numerical Analysis*, 58(2):1195–1216.

Jansen, M. J. W., Rossing, W. A. H., and Daamen, R. A. (1994). Monte Carlo estimation of uncertainty contributions from several independent multivariate sources. In Gasman, J. and van Straten, G., editors, *Predictability and nonlinear modelling in natural sciences and economics*, pages 334–343. Kluwer Academic Publishers.

L’Ecuyer, P. and Lemieux, C. (2002). A survey of randomized quasi-Monte Carlo methods. In Dror, M., L’Ecuyer, P., and Szidarovszki, F., editors, *Modeling Uncertainty: An Examination of Stochastic Theory, Methods, and Applications*, pages 419–474. Kluwer Academic Publishers.

Liu, R. and Owen, A. B. (2006). Estimating mean dimensionality of analysis of variance decompositions. *Journal of the American Statistical Association*, 101(474):712–721.

Mauntz, W. (2002). Global sensitivity analysis of general nonlinear systems. Master’s thesis, Imperial College.

Owen, A. B. (2003). The dimension distribution and quadrature test functions. *Statistica Sinica*, 13(1):1–17.

Owen, A. B. and Tribble, S. D. (2005). A quasi-Monte Carlo Metropolis algorithm. *Proceedings of the National Academy of Sciences*, 102(25):8844–8849.

Rohatgi, V. K. and Székely, G. (1989). Sharp inequalities between skewness and kurtosis. *Statistics & probability letters*, 8(4):297–299.

Saltelli, A. (2002). Making best use of model evaluations to compute sensitivity indices. *Computer Physics Communications*, 145:280–297.

Saltelli, A. and Sobol', I. M. (1995). About the use of rank transformation in sensitivity analysis of model output. *Reliability Engineering & System Safety*, 50(3):225–239.

Selvaraju, R. R., Cogswell, M., Das, A., Vedantam, R., Parikh, D., and Batra, D. (2017). Grad-cam: Visual explanations from deep networks via gradient-based localization. In *Proceedings of the IEEE International Conference on Computer Vision*, pages 618–626.

Sobol', I. M. (1990). On sensitivity estimation for nonlinear mathematical models. *Matematicheskoe Modelirovanie*, 2(1):112–118. (In Russian).

Sobol', I. M. (1993). Sensitivity estimates for nonlinear mathematical models. *Mathematical Modeling and Computational Experiment*, 1:407–414.

Yalcin, O. G. (2018). Image classification in 10 minutes with MNIST dataset. <https://towardsdatascience.com/imageclassification-in-10-minutes-with-mnist-dataset-54c35b77a38d>.

Yosinski, J., Clune, J., Nguyen, A., Fuchs, T., and Lipson, H. (2015). Understanding neural networks through deep visualization. Technical Report arXiv:1506.06579.

Appendix: Covariances under winding stairs

Winding stairs expressions are more complicated than the others and require somewhat different notation. Hence we employ some notation local to this appendix. For instance in winding stairs $\ell(i)$ has a special meaning as newly updated component of \mathbf{x}_i . Accordingly when we need a variable index other than j and k we use t instead of ℓ , in this appendix. We revert the t 's back to ℓ when quoting these theorems in the main body of the paper. Similarly, differences in function values are more conveniently described via which observation i is involved and not which variable. Accordingly, we work with Δ_i here instead of Δ_j in the main body of the article.

We begin with the regular winding stairs estimates and let $\Delta_i = f(\mathbf{x}_i) - f(\mathbf{x}_{i-1})$. For $i' > i$, the differences Δ_i and $\Delta_{i'}$ are independent if $\mathbf{x}_{i'-1}$ has no

common components with \mathbf{x}_i . This happens if $i' - 1 \geq i + d$, that is if $i' - i > d$. For any index i , the difference Δ_i may be dependent on $\Delta_{i'}$ for $-d < i' < d$ but no other $\Delta_{i'}$. It is not necessarily true that $\text{Cov}(\Delta_i^2, \Delta_{i+s}^2) = \text{Cov}(\Delta_i^2, \Delta_{i-s}^2)$ because different shared components of \mathbf{x} are involved in these two covariances.

The winding stairs estimate of $\tilde{\tau}_j^2$ is $\tilde{\tau}_j^2 = (1/(2N)) \sum_{i=1}^N \Delta_{d(i-1)+j}^2$. Because $\text{Cov}(\Delta_{i+d}^2, \Delta_{i'+d}^2) = \text{Cov}(\Delta_i^2, \Delta_{i'}^2)$, we find that for $1 \leq j < k \leq d$,

$$\text{Cov}(\tilde{\tau}_j^2, \tilde{\tau}_k^2) = \frac{1}{4N} \left(\text{Cov}(\Delta_{d+j}^2, \Delta_{d+k}^2) + \text{Cov}(\Delta_{2d+j}^2, \Delta_{d+k}^2) \right). \quad (17)$$

The disjoint winding stairs algorithm has

$$\text{Cov}(\tilde{\tau}_j^2, \tilde{\tau}_k^2) = \frac{1}{4N} \text{Cov}(\Delta_{d+j}^2, \Delta_{d+k}^2) \quad (18)$$

because Δ_{2d+j} has no z 's in common with Δ_{d+k} .

Theorem 3. *For the additive function f_A of (8),*

$$\text{Var}(\check{\delta}) = \frac{1}{N} \sum_{j=1}^d \left(2 + \frac{\kappa_j}{2} \right) \sigma_j^4 + \frac{N-1}{2N^2} \sum_{j=1}^d (\kappa_j + 2) \sigma_j^4 \quad (19)$$

$$\text{Var}(\ddot{\delta}) = \frac{1}{N} \sum_{j=1}^d \left(2 + \frac{\kappa_j}{2} \right) \sigma_j^4. \quad (20)$$

Proof. For an additive function under winding stairs

$$\begin{aligned} \Delta_{d(i-1)+j} &= g_j(\mathbf{x}_{d(i-1)+j,j}) - g_j(\mathbf{x}_{d(i-2)+j,j}) \\ &= g_j(z_{d(i-1)+j}) - g_j(z_{d(i-2)+j}) \end{aligned}$$

because $r(i, j) = d\lfloor (i-j)/d \rfloor + j$ yields $r(d(i-1) + j, j) = d(i-1) + j$. It follows that $\tilde{\tau}_j^2$ and $\tilde{\tau}_k^2$ have no z 's in common when $j \neq k$ and so they are independent. Now define the independent and identically distributed random variables $Y_i = g_j(z_{d(i-1)+j})$ for $i = 1, \dots, N$. Then

$$\begin{aligned} \text{Var}(\tilde{\tau}_j^2) &= \text{Var}\left(\frac{1}{2N} \sum_{i=1}^N (Y_i - Y_{i-1})^2\right) \\ &= \frac{1}{4N} \text{Var}((Y_1 - Y_0)^2) + \frac{N-1}{2N^2} \text{Cov}((Y_1 - Y_0)^2, (Y_2 - Y_1)^2) \\ &= \frac{(8+2\kappa_j)\sigma^4}{4N} + \frac{(N-1)(\kappa+2)\sigma^4}{2N^2} \end{aligned}$$

by Lemma 1, establishing (19). For disjoint winding squares all of the Δ_i are independent in the additive model establishing (20). \square

Next we turn to the multiplicative model $f_P(\mathbf{x}_i) = \prod_{j=1}^d g_j(z_{r(i,j)})$. A key distinction arises for variables ‘between’ the j ’th and k ’th and variables that are not between those. For $j < k$ the indices t between them are designated by $t \in (j, k)$ and the ones ‘outside’ of them are designated by $t \notin [j, k]$, meaning that $t \in \{1, \dots, j-1\} \cup \{k+1, \dots, d\}$.

Theorem 4. For the multiplicative function f_P of (9),

$$\begin{aligned} \text{Var}(\ddot{\delta}) &= \frac{1}{N} \sum_{j=1}^d \sigma_j^4 \left(\left(3 + \frac{\kappa_j}{2} \right) \prod_{t \neq j} \mu_{4t} - \prod_{t \neq j} \mu_{2t}^2 \right) \\ &+ \frac{2}{N} \sum_{j < k} \left(\frac{\eta_j \eta_k}{4} \prod_{t \in (j, k)} \mu_{2t}^2 \prod_{t \notin [j, k]} \mu_{4t} - \sigma_j^2 \sigma_k^2 \mu_{2j} \mu_{2k} \prod_{t \notin \{j, k\}} \mu_{2t}^2 \right) \end{aligned} \quad (21)$$

and

$$\text{Var}(\check{\delta}) = \text{Var}(\ddot{\delta}) + \frac{2}{N} \sum_{j < k} \left(\frac{\eta_j \eta_k}{4} \prod_{t \in (j, k)} \mu_{4t} \prod_{t \notin [j, k]} \mu_{2t}^2 - \sigma_j^2 \sigma_k^2 \mu_{2j} \mu_{2k} \prod_{t \notin \{j, k\}} \mu_{2t}^2 \right) \quad (22)$$

where $\eta_j = \mu_{4j} - 2\mu_j \mu_{3j} + \mu_{2j}^2$.

Proof. We use equation (18) to write covariances in terms of the first few \mathbf{x}_i . For $1 \leq j \leq d$ we have $\Delta_{d+j} = \prod_{t=1}^{j-1} g_t(z_{d+t}) \times (g_j(z_{d+j}) - g_j(z_d)) \times \prod_{t=j+1}^d g_t(z_t)$ so that

$$\mathbb{E}(\Delta_{d+j}^2) = 2\sigma_j^2 \prod_{t \neq j} \mu_{2t} \quad \text{and} \quad \mathbb{E}(\Delta_{d+j}^4) = (12 + 2\kappa_j) \sigma_j^4 \prod_{t \neq j} \mu_{4t}$$

and $\text{Var}(\Delta_{d+j}^2) = \eta_j \prod_{t \neq j} \mu_{4t} - 4\sigma_j^4 \prod_{t \neq j} \mu_{2t}^2$. Then for $1 \leq j < k \leq d$ and using a convention that empty products are one,

$$\begin{aligned} \mathbb{E}(\Delta_{d+j}^2 \Delta_{d+k}^2) &= \prod_{t=1}^{j-1} \mu_{4t} \times \eta_j \times \prod_{t=j+1}^{k-1} \mu_{2t}^2 \times \eta_k \times \prod_{t=k+1}^d \mu_{4t} \quad \text{and} \\ \mathbb{E}(\Delta_{2d+j}^2 \Delta_{d+k}^2) &= \prod_{t=1}^{j-1} \mu_{2t}^2 \times \eta_j \times \prod_{t=j+1}^{k-1} \mu_{4t} \times \eta_k \times \prod_{t=k+1}^d \mu_{2t}^2. \end{aligned}$$

Therefore,

$$\begin{aligned} \text{Cov}(\Delta_{d+j}^2, \Delta_{d+k}^2) &= \eta_j \eta_k \prod_{t \in (j, k)} \mu_{2t}^2 \prod_{t \notin [j, k]} \mu_{4t} - 4\sigma_j^2 \sigma_k^2 \mu_{2j} \mu_{2k} \prod_{t \notin \{j, k\}} \mu_{2t}^2, \quad \text{and} \\ \text{Cov}(\Delta_{2d+j}^2, \Delta_{d+k}^2) &= \eta_j \eta_k \prod_{t \in (j, k)} \mu_{4t} \prod_{t \notin [j, k]} \mu_{2t}^2 \prod_{t=1}^{j-1} \mu_{2t}^2 - 4\sigma_j^2 \sigma_k^2 \mu_{2j} \mu_{2k} \prod_{t \notin \{j, k\}} \mu_{2t}^2. \end{aligned}$$

Putting these together establishes the theorem. \square